

# A highly thermostable and transparent lateral heat spreader based on silver nanowire/polyimide composite†

Junpeng Li,<sup>a</sup> Shuhua Qi,<sup>\*a</sup> Juan Li,<sup>b</sup> Mengyu Zhang<sup>a</sup> and Zhaofu Wang<sup>a</sup>

Heat accumulation is a severe problem for high-power light-emitting diodes (LEDs). Here, we introduce a thermostable and transparent lateral heat spreader as an additional heat-escaping channel of an LED chip to improve the thermal management of LED devices. The lateral heat spreader was prepared based on a silver nanowire (AgNW)/polyimide composite comprising a thin polyacrylate layer soldering a conductive AgNW network to confine the nanowires to the surface of a polyimide film and to obtain low contact resistance between the nanowires. The AgNW/polyimide composite film has a figure-of-merit sheet resistance of 7 ohm sq<sup>-1</sup> with 76% transmittance at 550 nm. After heating at 200 °C for 168 h, the sheet resistance increases to 16 ohm sq<sup>-1</sup>. The thermal conductivity and thermal diffusivity are 130.2 W m<sup>-1</sup> K<sup>-1</sup> and 60.5 mm<sup>2</sup> s<sup>-1</sup>, respectively, which are comparable to those of a commercial copper foil. A demonstration shows the core temperature in a thermal diffusion apparatus can be lowered by 9 °C. The experimental data combined with computational simulation indicate the Joule heating could be drawn away efficiently along the lateral heat spreader.

The light-emitting diode (LED), a semiconductor component with different energy gaps emitting visible light of different colors, has witnessed rapid advancements in general lighting as a replacement for conventional incandescent and fluorescent lamps due to its multiple advantages, such as low power consumption, highly efficient light generation, fast response time and long lifetime.<sup>1–5</sup> To achieve higher light output performance, higher driving current is the critical factor. However, LED devices operating at high driving current not only produce high lumens but also generate a significant amount of Joule heating at the p-n junction, which causes problems such as low illumination intensity, wavelength shift and short lifetime.<sup>1,6,7</sup> To extract the heat generated in an LED chip, a large number of methods have been used to improve heat dissipation. The conventional LED chip is assembled on a substrate board and encapsulated by a transparent material. The heat generated can be drawn away by thermal conduction along the substrate board and transparent encapsulation materials. Heat transmission along the substrate board is the major thermal management. As such, the use of vertical geometry on high thermal conductivity substrates was proposed to overcome heat accumulation.<sup>8,9</sup> A Cu heat spreader with Ag reflector was

designed to contact the LED substrate.<sup>5,6</sup> Scalable graphene oxide microscale patterns have been used as a micro heat-dissipating channel on LED substrates.<sup>1</sup> However, thermal conduction along the transparent encapsulation materials has not been reported. Due to the low thermal conductivity of the encapsulation materials, hotspots developed on the LED chip still persist.

Silver nanowire (AgNW)/polymer composites have attracted much attention due to their high visual transmittance and high surface conductivity, which could be applied as the encapsulation materials of a light-emitting surface.<sup>10–12</sup> Heat produced by an LED chip would spread out along the conductive AgNW network. We previously reported an AgNW/polyacrylate composite film, which can be subjected to a temperature as high as 200 °C without obvious conductive degradation. However, visual transmittance decreased due to thermal aging of the polyacrylate substrate.<sup>13</sup> Polyimide composites have been widely used due to their outstanding thermal stability, high glass transition temperature, good chemical resistance and superior mechanical properties.<sup>14–17</sup> A polyimide/boron nitride/graphene hybrid composite film exhibits a low coefficient of thermal expansion of 11 ppm K<sup>-1</sup>.<sup>18</sup> A shape memory composite based on polyimide and graphene can be used at 230 °C.<sup>19</sup> However, these polyimide composites without or with low visual transmittance cannot be applied as LED chip encapsulation materials.

In this work we report the fabrication of a transparent and thermostable composite comprising a conductive AgNW network soldered by a thin polyacrylate layer on the surface of a

<sup>a</sup>Department of Applied Chemistry, School of Science, Northwestern Polytechnical University, Xi'an, Shaanxi 710072, PR China. E-mail: qishuhua@nwpu.edu.cn

<sup>b</sup>Ningbo Institute of Material Technology and Engineering, Chinese Academy of Sciences, Ningbo, Zhejiang 315201, PR China

polyimide substrate. The AgNW/polyimide composite film with a sheet resistance of  $7 \text{ ohm sq}^{-1}$  can tolerate high temperature up to  $200^\circ\text{C}$  for 168 h, without obvious sheet resistance and visual transmittance degeneration being observed. As a lateral heat spreader, the thermal conduction of the composite film is comparable to that of a commercial copper foil. The heat spreader is introduced as an additional heat-escaping channel of the light-emitting surface of an LED chip. A demonstration shows a thermal diffusion apparatus with low core temperatures and high edge temperatures, compared to that without the lateral heat spreader, indicating that much more Joule heating is drawn away along the heat spreader rather than dissipating near the touching material.

## Results and discussion

Fig. 1 illustrates the fabrication of the AgNW/polyimide composite film. The process began with bar-coating AgNW on a glass release substrate, followed by spin-coating an acrylate(tris(2-hydroxy ethyl)isocyanurate triacrylate) solution in cyclopentanone. After UV curing, a thin polyacrylate coating was formed over the conductive AgNW network. A polyimide precursor solution was deposited and cured at  $150^\circ\text{C}$  under vacuum for 8 h. After the precursor copolymerization, the resulting composite film was peeled off the glass release substrate. The AgNW network was transferred into the thin intermediate polyacrylate layer bonded on the surface of the polyimide substrate.

The AgNW/polyimide composite was fabricated by drop-casting the polyimide precursor solution on the glass substrate with a preformed AgNW network. During the curing of the polyimide substrate, the AgNW network was immersed in the precursor solution with low viscosity at  $150^\circ\text{C}$  for 8 h under vacuum. Due to thermodynamics or Brownian motion, nanowires would relocate and detach from the glass substrate. As shown in Fig. 2(a), segments of the nanowires submerged into the polymer substrate, and distributed in a layer about 300 nm thick shown in the cross-sectional image. Therefore, the surface conductivity of the composite was low. A thin polyacrylate layer was employed to “solder” the nanowires together on the glass substrate. During curing of the polyimide film, the thin layer protected the AgNW network from intrusion by the polyimide

precursor. AgNW soldered by the thin layer cannot move. In the resulting composite, the entire AgNW network was enriched along the composite surface as shown in Fig. 2(b), which would lead to a better surface conductivity than without the intermediate polyacrylate layer. For instance, by transferring the same coating density of AgNW on a glass release substrate, the composite film comprising the thin polyacrylate layer has a sheet resistance of  $7 \text{ ohm sq}^{-1}$ . However, the composite electrode without this intermediate layer shows a sheet resistance of  $565 \text{ ohm sq}^{-1}$  (see data in ESI Fig. S1†).

Bonding strength between AgNW and the polyacrylate layer, and between the polyacrylate layer and polyimide substrate is formed by hydrogen bonding and van der Waals interactions. The bonding strength was checked, as shown in Fig. S2.† After 1000 cycles of adhesion and peeling, only  $0.5 \text{ ohm}$  was measured, indicative of strong mechanical bonding between the AgNW network and thin polyacrylate layer, and between the thin polyacrylate layer and polyimide substrate as well. The resistance increase was measured because of the different contact points and the contact resistance during the measurement.

In the remaining discussions, we will focus on the composite film with the thin intermediate polyacrylate layer, and all composite films hereafter refer to this architecture.

The in-plane thermal diffusivity of the AgNW/polyimide composite films and a commercial copper foil was determined at room temperature using a laser flash method according to a previous report.<sup>20</sup> In Fig. 3 the composite film with lower sheet resistance has beneficial thermal conductivity due to more thermally conductive pathways formed with the AgNW network. Thermal diffusivity and thermal conductivity of the composite film with sheet resistance of  $7 \text{ ohm sq}^{-1}$  are  $60.5 \text{ mm}^2 \text{ s}^{-1}$  and  $130.2 \text{ W m}^{-1} \text{ K}^{-1}$ , which are comparable to those of copper foil of  $70.2 \text{ mm}^2 \text{ s}^{-1}$  and  $132.5 \text{ W m}^{-1} \text{ K}^{-1}$ , respectively. The polyimide film without AgNW network exhibited thermal conductivity as low as  $0.2 \text{ W m}^{-1} \text{ K}^{-1}$ . Table S1† provides detailed information about the AgNW/polyimide composites and the commercial copper foil employed in this research.

The AgNW network, as the thermally conductive pathway in the AgNW/polyimide composite, determines the overall thermal conductivity of the composite film. The thermal stability of the AgNW network in a composite film was checked, as shown in Fig. 4. The AgNW/polyimide composite film with an initial sheet resistance of  $7 \pm 1 \text{ ohm sq}^{-1}$  was heated on a hot plate at  $200^\circ\text{C}$ . After 168 h the sheet resistance increased to  $16 \pm 3 \text{ ohm sq}^{-1}$ . Thermal diffusivity and thermal conductivity were measured as  $59.1 \text{ mm}^2 \text{ s}^{-1}$  and  $129.1 \text{ W m}^{-1} \text{ K}^{-1}$ , respectively, which remain almost as high as those of a fresh composite film. For comparison, an AgNW network on a glass substrate lost its conductivity when subjected to  $200^\circ\text{C}$  for 120 min, as shown in Fig. S3.† The AgNW network embedded into the surface of the polymer substrate was protected by the polymer from oxidation at high temperature, so the composite film retained a low sheet resistance. The thermal stability of the polymer substrate is characterized in Fig. S4.† The glass transition temperatures of the polyacrylate layer and polyimide substrate are  $140^\circ\text{C}$  and  $260^\circ\text{C}$ , respectively, indicating a high thermal stability.

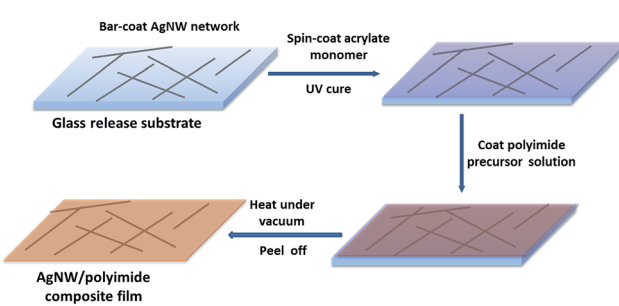
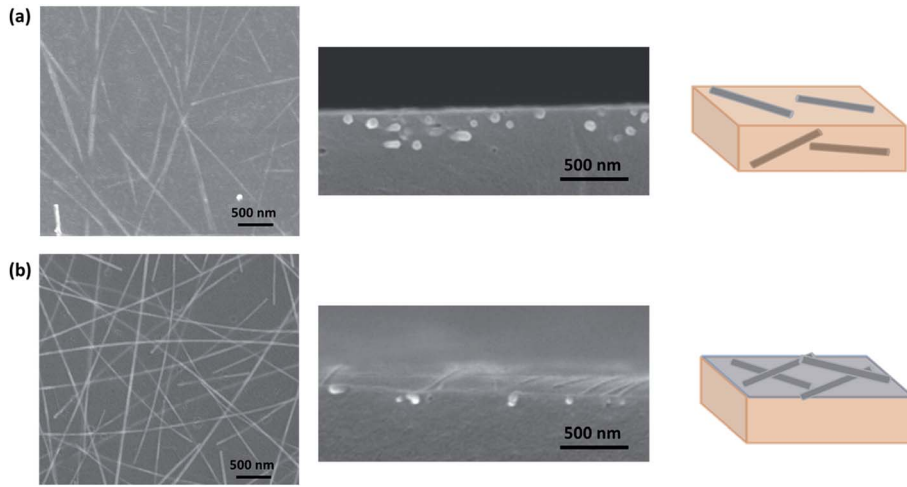
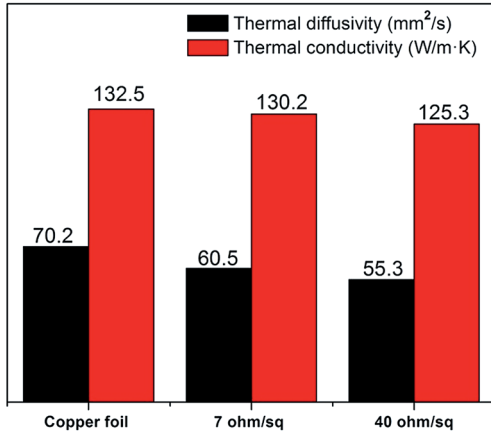


Fig. 1 Schematic illustration of the fabrication of AgNW/polyimide composite film. The thicknesses of the polyacrylate coating and AgNW/polyimide composite film are 90 nm and 50  $\mu\text{m}$ , respectively.



**Fig. 2** Distribution of AgNW in the surface of a polyimide polymer substrate without a thin polyacrylate layer (a) and with a thin polyacrylate layer (b). (a) SEM images of AgNW embedded in polyimide film (left) and the cross-section of the composite film (middle). Illustration of AgNW in polyimide substrate (right). (b) SEM images and illustration of the composite film with a thin polyacrylate layer.



**Fig. 3** Thermal diffusivity and thermal conductivity of copper foil and AgNW/polyimide composite films with sheet resistances of 7  $\text{ohm}\ \text{sq}^{-1}$  and 40  $\text{ohm}\ \text{sq}^{-1}$ .

Due to the low thermal conductivity of the polyimide substrate, most heat would transmit along the conductive AgNW network in the composite film. Thicker AgNW network would improve the thermally conductive path. However, the visual transmittance decreases. In Fig. 5 the transmittances at 550 nm for the pure polyimide film, and composite films with sheet resistances of 40  $\text{ohm}\ \text{sq}^{-1}$  and 7  $\text{ohm}\ \text{sq}^{-1}$  are 88%, 82% and 76%, respectively. After heating at 200 °C for 168 h, the initial transmittance of 76% at 550 nm decreased to 75%. The polyimide substrate showed a high thermal stability. Compared with an AgNW/polyacrylate conductor shown in Fig. S5,<sup>†13</sup> the initial transmittance of 77.7% decreased to 61.3% after heating at 200 °C for 168 h. The polyacrylate substrate broke down when exposed to a high temperature for a long time.

To evaluate the efficiency of lateral thermal spreading, a thermal diffusion apparatus is set up as shown in Fig. 6(a). A hemispherical thermal conductor with thermocouples

inserted inside is connected to an electronic thermometer. The three-dimensional model and profile schematic of the thermal diffusion apparatus are illustrated in Fig. 6(b) and (c). The dimension size and thermocouple positions are shown in Fig. S6.<sup>†</sup> The thermal diffusion apparatus is heated at 20 W by a heater. The inside temperature of the hemispherical thermal conductor with thermal conductivity of 0.15  $\text{W m}^{-1}\ \text{K}^{-1}$  is detected by seven thermocouples, as shown in Fig. 6(d). With the AgNW/polyimide composite film as a heat spreader, the temperatures from positions -1 to 1 are 115.2 °C, 117 °C and 115.5 °C, respectively, which are lower than those with a polyimide film, showing temperatures of 120 °C, 126 °C and 119 °C. The core temperature decreases by 9 °C. The edge temperatures at positions -3, -2, 2 and 3 are 102 °C, 110 °C, 110 °C and 101 °C, respectively, which are higher than those with a polyimide film showing temperatures of 92.3 °C, 105.4 °C, 105.7 °C and 95 °C.

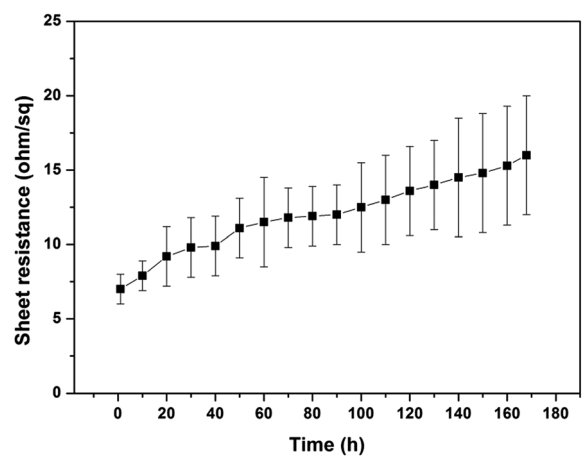


**Fig. 4** Transient sheet resistance of AgNW/polyimide composite film at 200 °C for 168 h. The composite film had an initial sheet resistance of 7  $\text{ohm}\ \text{sq}^{-1}$ .

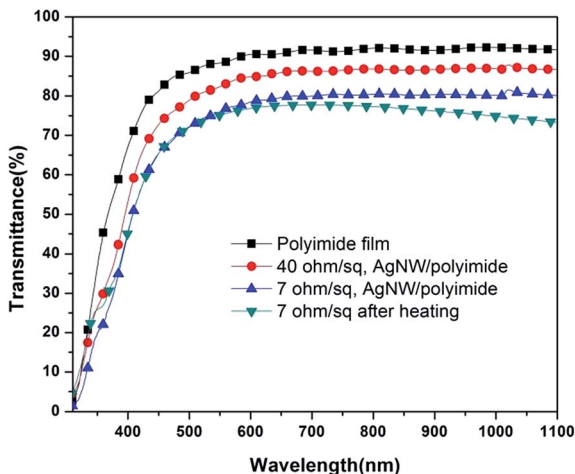


Fig. 5 Transmittance spectra of polyimide film and of composite films with different sheet resistances. The thickness of all films is 50  $\mu\text{m}$ .

The temperature propagation in the hemispherical thermal conductor is simulated using a finite-element method (see details in experimental section) and is shown in Fig. 6(e). The experimental and computational results indicate the heat

generated by the heater would spread out along the AgNW/polyimide composite film. More Joule heat would spread along the heat spreader and be dissipated by a heat sink along the edge of the lateral heat spreader. So the core temperature is low. The temperatures at the edge are high due to the heating by the lateral heat spreader. Heat along the heat spreader is mainly carried by free electrons of the AgNW network. Heat is transferred highly efficiently in the AgNW network, rather than polymer substrate, in which thermal conduction is dominated by acoustic phonons, ion-core vibration in a crystal lattice. Consequently, lateral heat transmission is faster than that along the longitudinal direction. Fig. 6(f) illustrates the heat flux density along the heat spreader is higher than that in a hemispherical thermal conductor, indicating that heat tends to transmit along the composite heat spreader.

## Conclusion

In summary, a transparent and thermostable lateral heat spreader has been prepared comprising an AgNW network on the surface of a polyimide substrate. Polyacrylate was introduced to “solder” the nanowire junctions to lower the nanowire–nanowire junction resistance, and to confine the AgNW percolation

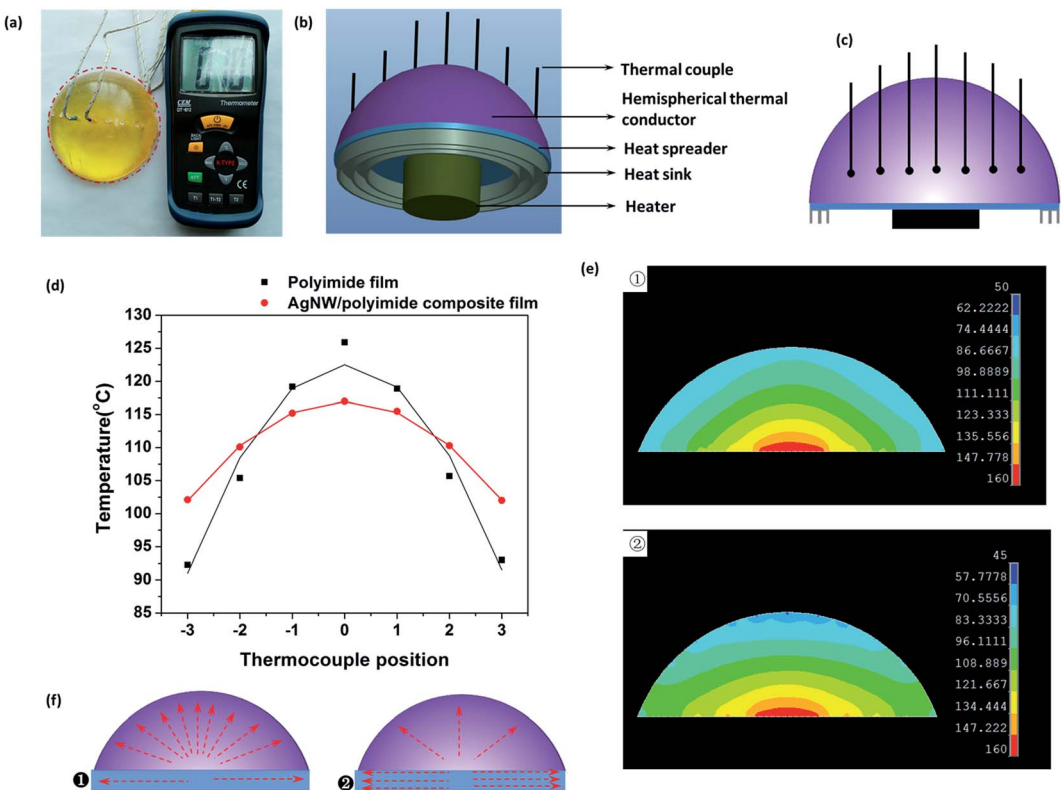


Fig. 6 (a) Photograph showing the thermal diffusion apparatus. One end of a thermocouple is inserted into the hemispherical thermal conductor; the other end is connected to a thermometer. The hemispherical thermal conductor is located by the red circle. (b) Three-dimensional model and (c) the vertical profile schematic of the thermal diffusion apparatus. The purple and blue areas represent the hemispherical thermal conductor and the heat spreader, respectively. A heat sink is attached along the edge of the lateral heat spreader. (d) Temperature profiles of the hemispherical thermal conductor when heating at 20 W. The temperature was detected by a thermocouple. (e) Simulated temperature distribution in the hemispherical thermal conductor (1) with a polyimide film or (2) with an AgNW/polyimide composite film as a lateral heat spreader. (f) Illustration of the heat flux density in the thermal diffusion apparatus (1) with a polyimide film and (2) with an AgNW/polyimide composite film as a heat spreader. Arrows indicate the heat flux direction and heat density.

network on the surface of the polyimide substrate. The resulting AgNW/polyimide composite film has a figure-of-merit sheet resistance of  $7 \text{ ohm sq}^{-1}$  with 76% transmittance at 550 nm. After heating at  $200^\circ\text{C}$  for 168 h, the sheet resistance increased to  $16 \text{ ohm sq}^{-1}$ . Thermal diffusivity and thermal conductivity of the AgNW/polyimide composite heat spreader are  $60.5 \text{ mm}^2 \text{ s}^{-1}$  and  $130.2 \text{ W m}^{-1} \text{ K}^{-1}$ , respectively, which are comparable to those of a commercial copper foil. A thermal diffusion apparatus is set up to evaluate the efficiency of lateral heat spreading. The experimental and computational results indicate that most Joule heat would spread along the AgNW/polyimide composite heat spreader, which decreases obviously the core temperature in the hemispherical thermal conductor.

## Experimental section

### Preparation of the thin polyacrylate layer

A monomer solution of 20 wt% concentration in cyclopentanone, consisting of SR368D (tris(2-hydroxy ethyl)isocyanurate tri-acrylate from Sartomer with excellent heat resistance), was spin-coated over the AgNW conductive network at 5000 rpm, for 1 min. The monomer coating was cured under a Dymax ultraviolet bulb, at a speed of 1 foot per minute for one pass. The thin coating was 90 nm thick, as measured by a Dektak profilometer.

### Preparation of AgNW/polyimide composite film

AgNW was synthesized with an average diameter of between 25 and 35 nm, and average length of between 10 and 20  $\mu\text{m}$ . A dispersion of AgNW (concentration of  $1.5 \text{ mg mL}^{-1}$ ) in isopropanol and methanol (volume ratio, 1 : 2) was coated on a glass substrate by a Meyer bar. A thin polyacrylate layer was coated over the AgNW. A solution of polyimide (10% concentration in dimethylacetamide), synthesized according to previous reports, was drop-cast onto the thin polyacrylate layer on a glass substrate.<sup>21-23</sup> The precursors in solution were copolymerized at  $150^\circ\text{C}$  under vacuum for 8 h. The resulting AgNW/polyimide composite film was peeled off the glass substrate.

### Characterization

Thermal conductivity was measured using the laser flash method. Transmittance spectra were recorded by a Shimadzu UV-1700 spectrophotometer. SEM was performed with a JEOL JSM-6701F scanning electron microscope. The electrical resistivity was measured using a four-point-probe measurement system with a silver paste as the contact pad.

### Setup of thermal diffusion apparatus

The AgNW/polyimide composite heat spreader was heated by a heater. An aluminum cooling fin was attached around the composite film to improve thermal diffusion. A hemispherical thermally conductive medium with a thermal conductivity of  $0.15 \text{ W m}^{-1} \text{ K}^{-1}$  was placed on the AgNW/polyimide composite heat spreader. Seven thermocouples were inserted into the hemispherical thermally conductive medium to detect the local temperatures. Commercial thermally conductive silicone grease was coated on all touch surfaces to decrease thermal resistance. Dimensions of all components are available in ESI Fig. S6.†

### Simulation of heat distribution

A finite-element method was used to study the thermal distribution in the hemispherical thermal conductor with each of polyimide film and AgNW/polyimide composite film as the lateral heat spreader. The surface temperature is measured by an infrared image system. Heat radiation and heat convection are neglected during the simulation with Ansys software.

## References

- N. Han, T. V. Cuong, M. Han, B. D. Ryu, S. Chandramohan, J. B. Park, J. H. Kang, Y. J. Park, K. B. Ko, H. Y. Kim, H. K. Kim, J. H. Ryu, Y. S. Katharria, C. J. Choi and C. H. Hong, *Nat. Commun.*, 2013, **4**, 1452.
- S. Pimplikar, J. S. Speck, S. P. DenBaars and S. Nakamura, *Nat. Photonics*, 2009, **3**, 179–181.
- F. A. Ponce and D. P. Bour, *Nature*, 1997, **386**, 351.
- E. F. Schubert and J. K. Kim, *Science*, 2005, **308**, 1274.
- Y. Taniyasu, M. Kasu and T. Makimoto, *Nature*, 2006, **441**, 325.
- R. H. Horng, C. C. Chiang, H. Y. Hsiao, X. Zheng, D. S. Wuu and H. I. Lin, *Appl. Phys. Lett.*, 2008, **93**, 111907.
- Z. Yan, G. Liu, J. M. Khan and A. A. Balandin, *Nat. Commun.*, 2012, **3**, 827.
- C. F. Chu, F. I. Lai, J. T. Chu, C. C. Yu, C. F. Lin, H. C. Kuo and S. C. Wang, *J. Appl. Phys.*, 2004, **95**, 3916.
- H. Kim, K.-K. Kim, K.-K. Choi, H. Kim, J.-O. Song, J. Cho, K. H. Baik, C. Sone, Y. Park and T.-Y. Seong, *Appl. Phys. Lett.*, 2007, **91**, 23510.
- J. Li, J. Liang, L. Li, F. Ren, W. Hu, J. Li, S. Qi and Q. Pei, *ACS Nano*, 2014, **8**, 12874–12882.
- J. Liang, L. Li, X. Niu, Z. Yu and Q. Pei, *Nat. Photonics*, 2013, **7**, 817.
- Q. Xu, W. Shen, Q. Huang, Y. Yang, R. Tan, K. Zhu, N. Dai and W. Song, *J. Mater. Chem. C*, 2014, **2**, 3750.
- J. Li, J. Liang, X. Jian, W. Hu, J. Li and Q. Pei, *Macromol. Mater. Eng.*, 2014, **299**, 1403.
- D. Chen, H. Zhu and T. Liu, *ACS Appl. Mater. Interfaces*, 2010, **2**, 3702.
- D. Hill, Y. Lin, L. W. Qu, A. Kitaygorodskiy, J. W. Connell, L. F. Allard and Y. P. Sun, *Macromolecules*, 2005, **38**, 7670.
- J. Longun and J. O. Iroh, *Carbon*, 2012, **50**, 1823.
- Y. Liu, D. Peng, G. He, S. Wang, Y. Li, H. Wu and Z. Jiang, *ACS Appl. Mater. Interfaces*, 2014, **6**, 13051.
- M.-H. Tsai, I. H. Tseng, J.-C. Chiang and J.-J. Li, *ACS Appl. Mater. Interfaces*, 2014, **6**, 8639.
- M. Yoonessi, Y. Shi, D. A. Scheiman, M. Lebron-Colon, D. M. Tigelaar, R. A. Weiss and M. A. Meador, *ACS Nano*, 2012, **6**, 7644.
- Q.-Q. Kong, Z. Liu, J.-G. Gao, C.-M. Chen, Q. Zhang, G. Zhou, Z.-C. Tao, X.-H. Zhang, M.-Z. Wang, F. Li and R. Cai, *Adv. Funct. Mater.*, 2014, **24**, 4222.
- G. Chen, X. Pei, J. Liu and X. Fang, *J. Polym. Res.*, 2013, **20**, 159.
- S.-H. Hsiao, W. Guo, T.-H. Tsai and Y.-T. Chiu, *J. Polym. Res.*, 2014, **21**, 391.
- N.-H. You, Y. Suzuki, D. Yorifuji, S. Ando and M. Ueda, *Macromolecules*, 2008, **41**, 6361.